Title	Stabilized plane and axisymmetric piezoelectric finite element models
Author(s)	Sze, KY; Yang, XM; Yao, LQ
Citation	Finite Elements In Analysis And Design, 2004, v. 40 n. 9-10, p. 1105-1122
Issued Date	2004
URL	http://hdl.handle.net/10722/54311
Rights	Creative Commons: Attribution 3.0 Hong Kong License

Stabilized Plane and Axisymmetric Piezoelectric Finite Element Models

K.Y.Sze[1*], X.-M.Yang[1], L.-Q.Yao[2]

[1]Department of Mechanical Engineering, The University of Hong Kong, Pokfulam Road, Hong Kong, P.R.CHINA.

[2]Department of Mathematics, Suzhou University, Jiangsu Province 215006, P.R.CHINA.

ABSTRACT

This paper derives a four-node plane, a nine-node plane and a four-node axisymmetric stabilized elements for piezoelectric analysis. All elements are formulated by a stabilization approach founded on the generalized Hellinger-Reissner functional which employs stress, electric displacement, displacement and electric potential as the independent field variables. The lower and higher order stress and electric displacement are chosen to be orthogonal such that their coupling terms in the electromechanical flexibility matrices vanish. In the absence of the higher order modes, the elements are equivalent to their uniformly reduced integrated counterparts. Numerical examples are presented to illustrate that the stabilized elements are markedly more accurate than the standard fully integrated elements.

Keywords : finite element method, hybrid, stabilization, piezoelectric, electromechanical

* Corresponding author. Email: kysze@hku.hk

Published in Finite Elements in Analysis and Design 40 (2004) 1105–1122

1. Introduction

Piezoelectrics have been indispensable for frequency generators, sensors, actuators and adaptive structures. Owing to the complexity of the governing equations in piezoelectricity, closed form solutions for practical problems are very limited. Since Allik & Hughes presented their work of applying the electromechanical virtual work principle to finite element formulation [1], the method has been the dominating tool for analysis and design of piezoelectric devices and adaptive structures. In the principle, the *electromechanical displacement* which is the union of displacement and electric potential is the only field variables. Since none of the displacement and electric potential can be condensed from the principle, the formulation is irreducible [2]. Inheriting the work of Allik & Hughes, most of the finite element models in the literature are based on the irreducible formulation [3-15]. Unfortunately, they are often found to be inaccurate and susceptible to mesh distortion. To alleviate these shortcomings, the bubble/incompatible displacement method have been employed for three-dimensional element formulation [9,11,12]. Besides bubble/incompatible displacement method, hybrid or reducible variational principles have recently been employed to formulate piezoelectric finite element models for phase transformation, two-dimensional, three-dimensional, plate/shell and smart structure analyses [16-20]. While it is difficult to trace the origin of hybrid variational principles for piezoelectricity, the work of EerNisse is probably one of the earliest documentation [21]. By relaxing the constitutive, strain-displacement and/or electric field-electric potential relations, various hybrid variational functionals containing stress, strain, electric field and/or electric displacement as independent field variables in addition to electromechanical displacement can be derived [17,21].

In this paper, hybrid-stabilized quadrilateral elements for plane and axisymmetric piezoelectric analysis are proposed. The generalized Hellinger-Reissner's functional is employed. The functional involves the *electromechanical stress* which is the union of stress and electric displacement and the electromechanical displacement as the independently field variables. While the assumed electromechanical stress modes can be condensed at the element level, the condensation cost is considerably reduced by using orthogonal lower and higher order modes analogous to the lower and higher order orthogonal stress modes in admissible matrix formulation [22-25]. It will be seen that the lower order modes give rise to the uniformly reduced integrated or URI element and the higher order modes play the role of the stabilizing the communicable spurious zero energy modes. In other words, the lower order modes incur no condensation cost. Numerical examples show that the proposed elements are markedly more accurate than the fully integrated standard elements.

2. Formulation of Conventional and Stabilized Piezoelectric Elements

The following vectors of electromechanical displacement $\underline{v}$, electromechanical strain $\underline{\gamma}$ and

electromechanical stress $\underline{\tau}$ are introduced:

$$\underline{v} = \begin{Bmatrix} \underline{u} \\ \phi \end{Bmatrix} \ , \ \underline{\gamma} = \begin{Bmatrix} \underline{\varepsilon} \\ -\underline{E} \end{Bmatrix} \ , \ \underline{\tau} = \begin{Bmatrix} \underline{\sigma} \\ \underline{D} \end{Bmatrix} \tag{1}$$

in which $\underline{u}$, ϕ, $\underline{\varepsilon}$, $\underline{E}$, $\underline{\sigma}$ and $\underline{D}$ are the displacement, electric potential, vector of strain components, electric field, vector of stress components and electric displacement, respectively. The electromechanical strain-displacement and constitutive relations can be expressed as:

$$\underline{\gamma} = \underline{\underline{\mathscr{D}}}\,\underline{v} \ , \ \underline{\tau} = \underline{\underline{C}}\,\underline{\gamma} = \underline{\underline{C}}(\underline{\underline{\mathscr{D}}}\,\underline{v}) \tag{2}$$

where $\underline{\underline{\mathscr{D}}}$ is the electromechanical strain-displacement operator and $\underline{\underline{C}}$ is the electromechanical constitutive matrix. The latter can be partitioned as:

$$\underline{\underline{C}} = \begin{bmatrix} \underline{\underline{c}} & \underline{\underline{e}}^T \\ \underline{\underline{e}} & -\underline{\underline{\in}} \end{bmatrix} \tag{3}$$

where $\underline{\underline{c}}$ is the elasticity matrix, $\underline{\underline{e}}$ is the piezoelectric matrix and $\underline{\underline{\in}}$ is the dielectric matrix. Throughout this paper, single- and double-underlined items are respectively vectors and matrices.

For finite element formulation, the stationary condition of the following electromechanical potential energy functional can be employed [1]:

$$\Pi = \sum_e \frac{1}{2} \langle (\underline{\underline{\mathscr{D}}}\,\underline{v})^T \underline{\underline{C}} (\underline{\underline{\mathscr{D}}}\,\underline{v}) \rangle - P \tag{4}$$

where

$\langle \circ \rangle = \int_{\Omega^e} \circ \, d\Omega$ denotes the integral operator over the element domain Ω^e

Furthermore, e denotes element and P stands for the electromechanical load potential which includes the contribution from the surface traction, body force and surface charge. Prerequisites of the functional are the inter-element compatibility and essential boundary conditions on $\underline{v}$. Using the standard parametric interpolation, the electromechanical displacement and strain for the m-node plane or axisymmetric element can be expressed as:

$$\underline{v} = [N_1 \underline{\underline{I}}_3, ..., N_m \underline{\underline{I}}_3] \begin{Bmatrix} \underline{v}_1 \\ \vdots \\ \underline{v}_m \end{Bmatrix} = [N_1 \underline{\underline{I}}_3, ..., N_m \underline{\underline{I}}_3] \underline{q} \ , \ \underline{\gamma} = \underline{\underline{\mathscr{D}}}\,\underline{v} = (\underline{\underline{\mathscr{D}}}[N_1 \underline{\underline{I}}_3, ..., N_m \underline{\underline{I}}_3]) \underline{q} = \underline{\underline{B}}\,\underline{q} \tag{5}$$

in which $\underline{\underline{I}}_j$ denotes the j-th order identity matrix, N_i's are the interpolation functions, $\underline{v}_i$ is electromechanical displacement at the i-th node, $\underline{q}$ is the element electromechanical displacement vector and $\underline{\underline{B}}$ is the electromechanical strain-displacement matrix. Substituting (5) into (4),

$$\Pi = \sum_e \frac{1}{2} \underline{q}^T \underline{\underline{K}} \underline{q} - P \tag{6}$$

where

$$\underline{\underline{K}} = \langle \underline{\underline{B}}^T \underline{\underline{C}} \underline{\underline{B}} \rangle$$

is the conventional electromechanical element stiffness matrix. The reduced- and fully-integrated counterparts of $\underline{\underline{K}}$ can be expressed as:

$$\underline{\underline{K}}_R = \langle \underline{\underline{B}}^T \underline{\underline{C}} \underline{\underline{B}} \rangle_R \ , \ \underline{\underline{K}}_F = \langle \underline{\underline{B}}^T \underline{\underline{C}} \underline{\underline{B}} \rangle_F \tag{7}$$

in which $\langle \circ \rangle_R$ and $\langle \circ \rangle_F$ are the element domain integration operators that employ the reduced and full order quadratures, respectively.

By relaxing the last relation in (2), the following generalized Hellinger-Reissner functional can be obtained:

$$\Pi_{HR} = \sum_e \langle -\frac{1}{2} \underline{\tau}^T \underline{\underline{C}}^{-1} \underline{\tau} + \underline{\tau}^T (\underline{\underline{\mathcal{D}}} \underline{v}) \rangle - P \, . \tag{8}$$

The following form of the independently assumed electromechanical stress is assumed:

$$\underline{\tau} = \underline{\underline{P}}_L \underline{\beta}_L + \underline{\underline{P}}_H \underline{\beta}_H = [\underline{\underline{P}}_L \quad \underline{\underline{P}}_H] \begin{Bmatrix} \underline{\beta}_L \\ \underline{\beta}_H \end{Bmatrix} \tag{9}$$

in which $\underline{\underline{P}}$'s are the shape function matrices, $\underline{\beta}$'s are vectors of coefficients, L stands for lower order modes and H stands for higher order modes. With (5) and (9) invoked, the functional becomes:

$$\Pi_{HR} = \sum_e (-\frac{1}{2} \begin{Bmatrix} \underline{\beta}_L \\ \underline{\beta}_H \end{Bmatrix}^T \underline{\underline{H}} \begin{Bmatrix} \underline{\beta}_L \\ \underline{\beta}_H \end{Bmatrix} + \begin{Bmatrix} \underline{\beta}_L \\ \underline{\beta}_H \end{Bmatrix}^T \underline{\underline{G}} \underline{q}) - P \tag{10}$$

where

$$\underline{\underline{H}} = \begin{bmatrix} \langle \underline{\underline{P}}_L^T \underline{\underline{C}}^{-1} \underline{\underline{P}}_L \rangle & \langle \underline{\underline{P}}_L^T \underline{\underline{C}}^{-1} \underline{\underline{P}}_H \rangle \\ \langle \underline{\underline{P}}_H^T \underline{\underline{C}}^{-1} \underline{\underline{P}}_L \rangle & \langle \underline{\underline{P}}_H^T \underline{\underline{C}}^{-1} \underline{\underline{P}}_H \rangle \end{bmatrix} \text{ and } \underline{\underline{G}} = \begin{bmatrix} \langle \underline{\underline{P}}_L^T \underline{\underline{B}} \rangle \\ \langle \underline{\underline{P}}_H^T \underline{\underline{B}} \rangle \end{bmatrix}$$

are respectively the *electromechanical flexibility matrix* and *electromechanical leverage matrix*. In hybrid-stabilization which aims at improving the computational efficiency of hybrid elements [23-25], $\underline{\underline{P}}$'s are chosen such that

$$\langle \underline{\underline{P}}_L^T \underline{\underline{B}} \rangle^T \langle \underline{\underline{P}}_L^T \underline{\underline{C}}^{-1} \underline{\underline{P}}_L \rangle^{-1} \langle \underline{\underline{P}}_L^T \underline{\underline{B}} \rangle = \underline{\underline{K}}_R \ , \tag{11}$$

$$\langle \underline{\underline{P}}_L^T \underline{\underline{C}}^{-1} \underline{\underline{P}}_H \rangle = \underline{\underline{0}} \, . \tag{12}$$

By virtue of the last two equations and the stationary nature of the functional with respect to $\underline{\beta}$'s,

$$\langle \underline{\underline{P}}_L^T \underline{\underline{C}}^{-1} \underline{\underline{P}}_L \rangle \underline{\beta}_L = \langle \underline{\underline{P}}_L^T \underline{\underline{B}} \rangle \underline{q} \ , \ \langle \underline{\underline{P}}_H^T \underline{\underline{C}}^{-1} \underline{\underline{P}}_H \rangle \underline{\beta}_H = \langle \underline{\underline{P}}_H^T \underline{\underline{B}} \rangle \underline{q} \, , \ \Pi_{HR} = \sum_e (\frac{1}{2} \underline{q}^T \underline{\underline{K}}_S \underline{q}) - P \tag{13}$$

where

$$\underline{\underline{K}}_S = \underline{\underline{K}}_R + \langle \underline{\underline{P}}_H^T \underline{\underline{B}} \rangle^T \langle \underline{\underline{P}}_H^T \underline{\underline{C}}^{-1} \underline{\underline{P}}_H \rangle^{-1} \langle \underline{\underline{P}}_H^T \underline{\underline{B}} \rangle$$

is the stabilized *electromechanical stiffness matrix* and $\langle \underline{\underline{B}}^T \underline{\underline{P}}_H \rangle \langle \underline{\underline{P}}_H^T \underline{\underline{C}}^{-1} \underline{\underline{P}}_H \rangle^{-1} \langle \underline{\underline{P}}_H^T \underline{\underline{B}} \rangle$ is the stabilization matrix for the reduced-integrated matrix $\underline{\underline{K}}_R$. In this light, the higher order electromechanical stress modes must be chosen with respect to the communicable zero energy mode of $\underline{\underline{K}}_R$.

For all the elements to be proposed, their higher order electromechanical stress shape function matrix can be partitioned and expressed as:

$$\underline{\underline{P}}_H = [f_1 \underline{\underline{P}}_1 \mid f_2 \underline{\underline{P}}_2] \tag{14}$$

in which f's are functions of the parametric coordinates whereas $\underline{\underline{P}}_1$ and $\underline{\underline{P}}_2$ are independent of the parametric coordinates. With the above $\underline{\underline{P}}_H$,

$$\underline{\underline{K}}_S = \underline{\underline{K}}_R + \begin{bmatrix} \underline{\underline{P}}_1^T \langle f_1 \underline{\underline{B}} \rangle \\ \underline{\underline{P}}_2^T \langle f_2 \underline{\underline{B}} \rangle \end{bmatrix}^T \begin{bmatrix} \langle f_1^2 \rangle \underline{\underline{P}}_1^T \underline{\underline{C}}^{-1} \underline{\underline{P}}_1 & \langle f_1 f_2 \rangle \underline{\underline{P}}_1^T \underline{\underline{C}}^{-1} \underline{\underline{P}}_2 \\ \langle f_1 f_2 \rangle \underline{\underline{P}}_2^T \underline{\underline{C}}^{-1} \underline{\underline{P}}_1 & \langle f_2^2 \rangle \underline{\underline{P}}_2^T \underline{\underline{C}}^{-1} \underline{\underline{P}}_2 \end{bmatrix}^{-1} \begin{bmatrix} \underline{\underline{P}}_1^T \langle f_1 \underline{\underline{B}} \rangle \\ \underline{\underline{P}}_2^T \langle f_2 \underline{\underline{B}} \rangle \end{bmatrix} \tag{15}$$

An admissible change that does not trigger patch test failure and affect the element rank is to treat $\langle f_1 f_2 \rangle$ as zero [22,25]. Thus,

$$\underline{\underline{K}}_S = \underline{\underline{K}}_R + \sum_{m=1}^{2} \frac{1}{\langle f_m^2 \rangle} \langle f_m \underline{\underline{B}} \rangle^T \underline{\underline{P}}_m (\underline{\underline{P}}_m^T \underline{\underline{C}}^{-1} \underline{\underline{P}}_m)^{-1} \underline{\underline{P}}_m^T \langle f_m \underline{\underline{B}} \rangle \tag{16}$$

In order that element accuracy and legitimacy are least affected by discarding $\langle f_1 f_2 \rangle$, f's will be chosen such that $\langle f_1 f_2 \rangle$ is approximately zero as far as possible.

3. Four-Node Piezoelectric Stabilized Plane Element

For plane piezoelectricity defined with respect to the x-y-plane, the electromechanical displacement $\underline{v}$, strain $\underline{\gamma}$, stress $\underline{\tau}$ and strain-displacement operator are:

$$\underline{v} = \begin{Bmatrix} u_x \\ u_y \\ \phi \end{Bmatrix}, \ \underline{\gamma} = \begin{Bmatrix} \varepsilon_{xx} \\ \varepsilon_{yy} \\ 2\varepsilon_{xy} \\ -E_x \\ -E_y \end{Bmatrix}, \ \underline{\tau} = \begin{Bmatrix} \sigma_{xx} \\ \sigma_{yy} \\ \sigma_{xy} \\ D_x \\ D_y \end{Bmatrix}, \ \underline{\underline{\mathcal{D}}} = \begin{bmatrix} \partial/\partial x & 0 & 0 \\ 0 & \partial/\partial y & 0 \\ \partial/\partial y & \partial/\partial x & 0 \\ 0 & 0 & \partial/\partial x \\ 0 & 0 & \partial/\partial y \end{bmatrix} \tag{17}$$

For quadrilateral elements with parametric coordinates ξ and η, the following Jacobian matrix and its determinant can be derived:

$$\underline{\underline{J}} = \begin{bmatrix} x_{,\xi} & y_{,\xi} \\ x_{,\eta} & y_{,\eta} \end{bmatrix}, \; J = \det(\underline{\underline{J}}) = x_{,\xi}\, y_{,\eta} - x_{,\eta}\, y_{,\xi} \tag{18}$$

using which the integral over the element domain can be written as:

$$\langle \circ \rangle = \int_{\Omega^e} \circ d\Omega = \int_{-1}^{+1}\int_{-1}^{+1} \circ J d\xi d\eta \tag{19}$$

For the four-node plane element, the Jacobian determinant and the electromechanical strain-displacement matrix, see Figure 1, can be expressed as:

$$J = J_0 + J_1\xi + J_2\eta \;, \; \underline{\underline{B}} = \frac{1}{4J}(\underline{\underline{B}}_0 + \xi\underline{\underline{B}}_1 + \eta\underline{\underline{B}}_2) \tag{20}$$

in which J_0, J_1, J_2, $\underline{\underline{B}}_0$, $\underline{\underline{B}}_1$ and $\underline{\underline{B}}_2$ are independent of the ξ and η [26]. The reduced-integrated element is evaluated by the first order quadature and is equal to:

$$\underline{\underline{K}}_R = \langle \underline{\underline{B}}^T \underline{\underline{C}}\underline{\underline{B}} \rangle_1 = [\frac{1}{4J}(\underline{\underline{B}}_0 + \xi\underline{\underline{B}}_1 + \eta\underline{\underline{B}}_2)^T \underline{\underline{C}}(\underline{\underline{B}}_0 + \xi\underline{\underline{B}}_1 + \eta\underline{\underline{B}}_2)]\big|_{\xi=\eta=0} = \frac{1}{4J_0}\underline{\underline{B}}_0^T \underline{\underline{C}}\underline{\underline{B}}_0 \tag{21}$$

in which $\langle \circ \rangle_m$ denotes the $\langle \circ \rangle$ that employs the m-th order quadrature.

For the stabilized four-node plane element, the lower order electromechanical stress shape function matrix taken to be the identity matrix, i.e.

$$\underline{\underline{P}}_L = \underline{\underline{I}}_5 \tag{22}$$

Thu,

$$\langle \underline{\underline{P}}_L^T \underline{\underline{C}}^{-1} \underline{\underline{P}}_L \rangle = 4J_0 \underline{\underline{C}}^{-1} \;, \; \langle \underline{\underline{P}}_L^T \underline{\underline{B}} \rangle = \underline{\underline{B}}_0 \;, \; \langle \underline{\underline{P}}_L^T \underline{\underline{B}} \rangle^T \langle \underline{\underline{P}}_L^T \underline{\underline{C}}^{-1} \underline{\underline{P}}_L \rangle^{-1} \langle \underline{\underline{P}}_L^T \underline{\underline{B}} \rangle = \frac{1}{4J_0}\underline{\underline{B}}_0^T \underline{\underline{C}}\underline{\underline{B}}_0 = \underline{\underline{K}}_R \tag{23}$$

and (11) is valid for the chosen $\underline{\underline{P}}_L$. When the element assumes the shape of a 2×2 square, it can be checked that the element possesses the following communicable zero energy modes:

$$\begin{Bmatrix} u_\xi \\ u_\eta \\ \phi \end{Bmatrix} = \xi\eta \begin{Bmatrix} \alpha_1 \\ \alpha_2 \\ \alpha_3 \end{Bmatrix} \tag{24}$$

where α's are coefficients. The relevant electromechanical strain is:

$$\begin{Bmatrix} u_{\xi,\xi} \\ u_{\eta,\eta} \\ u_{\xi,\eta} + u_{\eta,\xi} \\ \phi_{,\xi} \\ \phi_{,\eta} \end{Bmatrix} = \begin{bmatrix} \eta & 0 & 0 \\ 0 & \xi & 0 \\ \xi & \eta & 0 \\ 0 & 0 & \eta \\ 0 & 0 & \xi \end{bmatrix} \begin{Bmatrix} \alpha_1 \\ \alpha_2 \\ \alpha_3 \end{Bmatrix} \tag{25}$$

which vanishes at reduced order integration point $\xi = \eta = 0$. The above zero energy modes can be

suppressed by the following electromechanical stress modes:

$$\begin{Bmatrix} \sigma_\xi \\ \sigma_\eta \\ \sigma_{\xi\eta} \\ D_\xi \\ D_\eta \end{Bmatrix} = \begin{bmatrix} \eta & 0 & 0 & 0 \\ 0 & 0 & \xi & 0 \\ 0 & 0 & 0 & 0 \\ 0 & \eta & 0 & 0 \\ 0 & 0 & 0 & \xi \end{bmatrix} \begin{Bmatrix} \beta_1 \\ : \\ \beta_4 \end{Bmatrix} \tag{26}$$

where β's are coefficients. For general quadrilaterals, the electromechanical stress modes can be obtained from the above equation by the tensorial transformation evaluated at $\xi = \eta = 0$ [27]. With reference to (14), the higher order electromechanical stress shape function matrix are defined by having:

$$f_1 = \frac{\eta}{J},\ f_2 = \frac{\xi}{J}\ ,\ \underline{\underline{P}}_1 = \left(\begin{bmatrix} x_{,\xi}\, x_{,\xi} & 0 \\ y_{,\xi}\, y_{,\xi} & 0 \\ x_{,\xi}\, y_{,\xi} & 0 \\ 0 & x_{,\xi} \\ 0 & y_{,\xi} \end{bmatrix} \right)\Big|_{\xi=\eta=0},\ \underline{\underline{P}}_2 = \left(\begin{bmatrix} x_{,\eta}\, x_{,\eta} & 0 \\ y_{,\eta}\, y_{,\eta} & 0 \\ x_{,\eta}\, y_{,\eta} & 0 \\ 0 & x_{,\eta} \\ 0 & y_{,\eta} \end{bmatrix} \right)\Big|_{\xi=\eta=0}. \tag{27}$$

The reciprocal of J in f's is incorporated to satisfy (12). It can be noted that

$$\langle f_1 f_2 \rangle = \langle \frac{\xi\eta}{J^2} \rangle = \int_{-1}^{+1}\int_{-1}^{+1} \frac{\xi\eta}{J} d\xi d\eta \simeq \frac{1}{J\big|_{\xi=\eta=0}} \int_{-1}^{+1}\int_{-1}^{+1} \xi\eta d\xi d\eta = 0 \tag{28}$$

4. Nine-Node Piezoelectric Stabilized Plane Element

Figure 1 also shows the nine-node element. The reduced-integrated plane element is evaluated by the second order quadrature, i.e.

$$\underline{\underline{K}}_R = \langle \underline{\underline{B}}^T \underline{\underline{C}} \underline{\underline{B}} \rangle_2 = \sum_{i=1}^{4} (J \underline{\underline{B}}^T \underline{\underline{C}} \underline{\underline{B}})_i = \underline{\underline{\mathbb{B}}}^T \underline{\underline{\mathbb{J}}} \underline{\underline{\mathbb{C}}} \underline{\underline{\mathbb{B}}} \tag{29}$$

where the subscript i designates the i-th integration point and

$$\underline{\underline{\mathbb{B}}} = [\underline{\underline{B}}_1^T, \underline{\underline{B}}_2^T, \underline{\underline{B}}_3^T, \underline{\underline{B}}_4^T]^T\ ,\ \underline{\underline{\mathbb{C}}} = \text{diag.}\{\underline{\underline{C}}, \underline{\underline{C}}, \underline{\underline{C}}, \underline{\underline{C}}\}\ ,\ \underline{\underline{\mathbb{J}}} = \text{diag.}\{J_1 \underline{\underline{I}}_5, J_2 \underline{\underline{I}}_5, J_3 \underline{\underline{I}}_5, J_4 \underline{\underline{I}}_5\} \tag{30}$$

When the lower order electromechanical stress shape function matrix is taken to be:

$$\underline{\underline{P}}_L = [\underline{\underline{I}}_5 \quad \xi \underline{\underline{I}}_5 \quad \eta \underline{\underline{I}}_5 \quad \xi\eta \underline{\underline{I}}_5], \tag{31}$$

$\langle \underline{\underline{P}}_L^T \underline{\underline{C}}^{-1} \underline{\underline{P}}_L \rangle$ and $\langle \underline{\underline{P}}_L^T \underline{\underline{B}} \rangle$ can be evaluated with the second order quadrature without losing rank, i.e.

$$\langle \underline{\underline{P}}_L^T \underline{\underline{C}}^{-1} \underline{\underline{P}}_L \rangle_2 = \sum_{i=1}^{4} (J \underline{\underline{P}}_L^T \underline{\underline{C}}^{-1} \underline{\underline{P}}_L)_i = \underline{\underline{\mathbb{P}}}^T \underline{\underline{\mathbb{J}}} \underline{\underline{\mathbb{C}}}^{-1} \underline{\underline{\mathbb{P}}}, \ \langle \underline{\underline{P}}_L^T \underline{\underline{B}} \rangle_2 = \sum_{i=1}^{4} (J \underline{\underline{P}}_L^T \underline{\underline{B}})_i = \underline{\underline{\mathbb{P}}}_L^T \underline{\underline{\mathbb{J}}} \underline{\underline{\mathbb{B}}} \tag{32}$$

in which

$$\underline{\underline{\mathbb{P}}} = [(\underline{\underline{P}}_L)_1^T, (\underline{\underline{P}}_L)_2^T, (\underline{\underline{P}}_L)_3^T, (\underline{\underline{P}}_L)_4^T]^T$$

For the chosen $\underline{\underline{P}}_L$, $\underline{\underline{\mathbb{P}}}$ is invertible,

$$\langle \underline{\underline{P}}_L^T \underline{\underline{B}} \rangle_2^T \langle \underline{\underline{P}}_L^T \underline{\underline{C}}^{-1} \underline{\underline{P}}_L \rangle_2^{-1} \langle \underline{\underline{P}}_L^T \underline{\underline{B}} \rangle_2 = (\underline{\underline{\mathbb{P}}}_L^T \underline{\underline{\mathbb{J}}} \underline{\underline{\mathbb{B}}})^T (\underline{\underline{\mathbb{P}}}^T \underline{\underline{\mathbb{J}}} \underline{\underline{\mathbb{C}}}^{-1} \underline{\underline{\mathbb{P}}})^{-1} (\underline{\underline{\mathbb{P}}}_L^T \underline{\underline{\mathbb{J}}} \underline{\underline{\mathbb{B}}}) = \underline{\underline{\mathbb{B}}}^T \underline{\underline{\mathbb{C}}} \underline{\underline{\mathbb{B}}} = \underline{\underline{K}}_R \tag{33}$$

and (11) is valid. When the element assumes the shape of a 2×2 square, it can be checked that the element possesses the following communicable zero energy modes [24]:

$$\begin{Bmatrix} u_\xi \\ u_\eta \\ \phi \end{Bmatrix} = (3\xi^2 - 1)(3\eta^2 - 1) \begin{Bmatrix} \alpha_1 \\ \alpha_2 \\ \alpha_3 \end{Bmatrix} \tag{34}$$

from which the electromechanical strain modes are:

$$\begin{Bmatrix} u_{\xi,\xi} \\ u_{\eta,\eta} \\ u_{\xi,\eta} + u_{\eta,\xi} \\ \phi_{,\xi} \\ \phi_{,\eta} \end{Bmatrix} = 6 \begin{bmatrix} p_1 & 0 & 0 \\ 0 & p_2 & 0 \\ p_2 & p_1 & 0 \\ 0 & 0 & p_1 \\ 0 & 0 & p_2 \end{bmatrix} \begin{Bmatrix} \alpha_1 \\ \alpha_2 \\ \alpha_3 \end{Bmatrix} \tag{35}$$

where $p_1 = \xi(3\eta^2 - 1)$ and $p_2 = \eta(3\xi^2 - 1)$. Both p's vanish at the reduced order integration point $\xi = \eta = \pm 1/\sqrt{3}$. The above modes can be suppressed by the following choice of electromechanical stress modes:

$$\begin{Bmatrix} \sigma_\xi \\ \sigma_\eta \\ \sigma_{\xi\eta} \\ D_\xi \\ D_\eta \end{Bmatrix} = \begin{bmatrix} p_1 & 0 & 0 & 0 \\ 0 & 0 & p_2 & 0 \\ 0 & 0 & 0 & 0 \\ 0 & p_1 & 0 & 0 \\ 0 & 0 & 0 & p_2 \end{bmatrix} \begin{Bmatrix} \beta_1 \\ : \\ \beta_4 \end{Bmatrix} \tag{36}$$

For a general quadrilateral, the electromechanical stress modes can be obtained from the above equation by the transformation evaluated at $\xi = \eta = 0$ []. With reference to (14), the higher order electromechanical stress shape function matrix are defined having:

$$f_1 = \frac{p_1}{J} \ , \ f_2 = \frac{p_2}{J} \tag{37}$$

whereas $\underline{\underline{P}}_1$ and $\underline{\underline{P}}_2$ for the present element are defined in the identical way as in (27). The reciprocal of J in f's is incorporated to satisfy (12). It can be noted that

$$\langle f_1 f_2 \rangle = \langle \frac{p_1 p_2}{J^2} \rangle = \int_{-1}^{+1}\int_{-1}^{+1} \frac{p_1 p_2}{J} d\xi d\eta \simeq \frac{1}{J|_{\xi=\eta=0}} \int_{-1}^{+1}\int_{-1}^{+1} p_1 p_2 d\xi d\eta = 0 \tag{38}$$

5. Four-Node Piezoelectric Stabilized Axisymmetric Element

For axisymmetric piezoelectricity defined with respect to the *r*-*z*-plane, the electromechanical displacement $\underline{v}$, strain $\underline{\gamma}$, stress $\underline{\tau}$ and strain-displacement operator are:

$$\underline{v} = \begin{Bmatrix} u_r \\ u_z \\ \phi \end{Bmatrix}, \ \underline{\gamma} = \begin{Bmatrix} \varepsilon_{\theta\theta} \\ \varepsilon_{rr} \\ \varepsilon_{zz} \\ 2\varepsilon_{rz} \\ -E_r \\ -E_z \end{Bmatrix}, \ \underline{\tau} = \begin{Bmatrix} \sigma_{\theta\theta} \\ \sigma_{rr} \\ \sigma_{zz} \\ \sigma_{rz} \\ D_r \\ D_z \end{Bmatrix}, \ \underline{\underline{\mathcal{D}}} = \begin{bmatrix} 1/r & 0 & 0 \\ \partial/\partial r & 0 & 0 \\ 0 & \partial/\partial z & 0 \\ \partial/\partial z & \partial/\partial r & 0 \\ 0 & 0 & \partial/\partial r \\ 0 & 0 & \partial/\partial z \end{bmatrix} \tag{39}$$

For quadrilateral elements with parametric coordinates ξ and η, the following Jacobian matrix and its determinant can be derived:

$$\underline{\underline{J}} = \begin{bmatrix} r_{,\xi} & z_{,\xi} \\ r_{,\eta} & z_{,\eta} \end{bmatrix}, \ J = \det(\underline{\underline{J}}) \tag{40}$$

The integral over the element domain can be written as:

$$\langle \circ \rangle = \int_{\Omega^e} \circ d\Omega = 2\pi \int_{-1}^{+1}\int_{-1}^{+1} \circ r J d\xi d\eta \tag{41}$$

For the four-node axisymmetric element, the interpolated radial coordinate, Jacobian determinant and electromechanical strain-displacement matrix can be expressed as:

$$r = a_0 + a_1\xi + a_2\eta + a_3\xi\eta \ , \ J = J_0 + J_1\xi + J_2\eta \ ,$$
$$\underline{\underline{B}} = \frac{1}{4J}\left(\begin{bmatrix} \frac{J}{r}\underline{\underline{M}}_0 \\ \underline{\underline{N}}_0 \end{bmatrix} + \xi \begin{bmatrix} \frac{J}{r}\underline{\underline{M}}_1 \\ \underline{\underline{N}}_1 \end{bmatrix} + \eta \begin{bmatrix} \frac{J}{r}\underline{\underline{M}}_2 \\ \underline{\underline{N}}_2 \end{bmatrix} + \xi\eta \begin{bmatrix} \frac{J}{r}\underline{\underline{M}}_3 \\ \underline{\underline{0}} \end{bmatrix} \right) \tag{42}$$

in which the row dimensions of $\underline{\underline{M}}$'s and $\underline{\underline{N}}$'s are respectively one and five whereas *a*'s and all entries of $\underline{\underline{M}}$'s and $\underline{\underline{N}}$'s are independent of ξ and η [28]. The reduced-integrated element is evaluated by the first order quadrature and is equal to:

$$\langle \underline{\underline{B}}^T \underline{\underline{C}} \underline{\underline{B}} \rangle_1 = [\frac{\pi r}{2J} \underline{\underline{B}}^T \underline{\underline{C}} \underline{\underline{B}}]\big|_{\xi=\eta=0} = \frac{\pi a_0}{2J_0} \begin{bmatrix} \frac{J_0}{a_0}\underline{\underline{M}}_0 \\ \underline{\underline{N}}_0 \end{bmatrix}^T \underline{\underline{C}} \begin{bmatrix} \frac{J_0}{a_0}\underline{\underline{M}}_0 \\ \underline{\underline{N}}_0 \end{bmatrix} \tag{43}$$

Unfortunately, this element fails the patch test as the first order quadrature cannot exactly integrate

the element volume and $\underline{\underline{B}}$ [22,25]. A remedy is to replace $\underline{\underline{B}}$ in the left hand side of the above expression with its domain average which can be obtained by the second order quadrature as:

$$\frac{1}{\langle 1\rangle_2}\langle \underline{\underline{B}}\rangle_2 = \frac{1}{4(3a_0J_0 + a_1J_1 + a_2J_2)}\begin{bmatrix} 3J_0\underline{\underline{M}}_0 + J_1\underline{\underline{M}}_1 + J_2\underline{\underline{M}}_2 \\ 3a_0\underline{\underline{N}}_0 + a_1\underline{\underline{N}}_1 + a_2\underline{\underline{N}}_2 \end{bmatrix} \tag{44}$$

The modified reduced-integrated element is:

$$\underline{\underline{K}}_R = \frac{1}{\langle 1\rangle_2}\langle \underline{\underline{B}}\rangle_2^T \underline{\underline{C}}\langle \underline{\underline{B}}\rangle_2 \tag{45}$$

For the stabilized axisymmetric four-node element, the lower order electromechanical stress shape function matrix is taken to be the identity matrix, i.e.

$$\underline{\underline{P}}_L = \underline{\underline{I}}_6 . \tag{46}$$

In this light,

$$\langle \underline{\underline{P}}_L^T \underline{\underline{C}}^{-1} \underline{\underline{P}}_L\rangle = \langle 1\rangle \underline{\underline{C}}^{-1} \ , \ \langle \underline{\underline{P}}_L^T \underline{\underline{B}}\rangle = \langle \underline{\underline{B}}\rangle \ ,$$

$$\langle \underline{\underline{B}}^T \underline{\underline{P}}_L\rangle\langle \underline{\underline{P}}_L^T \underline{\underline{C}}^{-1} \underline{\underline{P}}_L\rangle^{-1}\langle \underline{\underline{P}}_L^T \underline{\underline{B}}\rangle = \frac{1}{\langle 1\rangle}\langle \underline{\underline{B}}\rangle^T \underline{\underline{C}}\langle \underline{\underline{B}}\rangle = \underline{\underline{K}}_R , \tag{47}$$

and (11) is valid for the chosen $\underline{\underline{P}}_L$. When the element is a 2×2 square with its edges parallel to the *r*- or *z*-axes and its element origin at $r = r_0$, it can be checked that the element possesses the following communicable zero energy modes:

$$\begin{Bmatrix} u_\xi \\ u_\eta \\ \phi \end{Bmatrix} = \begin{bmatrix} \xi\eta & 0 & 0 & \eta \\ 0 & \xi\eta & 0 & -\xi \\ 0 & 0 & \xi\eta & 0 \end{bmatrix}\begin{Bmatrix} \alpha_1 \\ \vdots \\ \alpha_4 \end{Bmatrix} \tag{48}$$

where α's are coefficients. The relevant electromechanical strain is:

$$\begin{Bmatrix} u_\xi / r \\ u_{\xi,\xi} \\ u_{\eta,\eta} \\ u_{\xi,\eta} + u_{\eta,\xi} \\ \phi_{,\xi} \\ \phi_{,\eta} \end{Bmatrix} = \begin{Bmatrix} u_\xi /(r_0 + \xi) \\ u_{\xi,\xi} \\ u_{\eta,\eta} \\ u_{\xi,\eta} + u_{\eta,\xi} \\ \phi_{,\xi} \\ \phi_{,\eta} \end{Bmatrix} = \begin{bmatrix} \xi\eta/(r_0 + \xi) & 0 & 0 & \eta/(r_0 + \xi) \\ \eta & 0 & 0 & 0 \\ 0 & \xi & 0 & 0 \\ \xi & \eta & 0 & 0 \\ 0 & 0 & \eta & 0 \\ 0 & 0 & \xi & 0 \end{bmatrix}\begin{Bmatrix} \alpha_1 \\ \vdots \\ \alpha_4 \end{Bmatrix} \tag{49}$$

which vanishes at the reduced order integration point $\xi = \eta = 0$. The zero energy modes can be suppressed by the following higher order electromechanical stress modes:

$$\begin{Bmatrix} \sigma_\theta \\ \sigma_\xi \\ \sigma_\eta \\ \sigma_{\xi\eta} \\ D_\xi \\ D_\eta \end{Bmatrix} = \begin{bmatrix} \eta & 0 & 0 & \xi & 0 & 0 \\ 0 & \eta & 0 & 0 & 0 & 0 \\ 0 & 0 & 0 & 0 & \xi & 0 \\ 0 & 0 & 0 & 0 & 0 & 0 \\ 0 & 0 & \eta & 0 & 0 & 0 \\ 0 & 0 & 0 & 0 & 0 & \xi \end{bmatrix} \begin{Bmatrix} \beta_1 \\ \vdots \\ \beta_6 \end{Bmatrix} \tag{50}$$

For a general quadrilateral, the electromechanical stress modes can be obtained from the above equation by the tensorial transformation evaluated at $\xi = \eta = 0$ [29]. With reference to (14), the higher order electromechanical stress shape function matrix are defined by having:??

$$f_1 = \frac{\eta - \overline{\eta}}{J},\ f_2 = \frac{\xi - \overline{\xi}}{J},\ \underline{\underline{P}}_1 = \left(\begin{bmatrix} 1 & 0 & 0 \\ 0 & r_{,\xi} r_{,\xi} & 0 \\ 0 & z_{,\xi} z_{,\xi} & 0 \\ 0 & r_{,\xi} z_{,\xi} & 0 \\ 0 & 0 & r_{,\xi} \\ 0 & 0 & z_{,\xi} \end{bmatrix} \right)\Big|_{\xi=\eta=0},\ \underline{\underline{P}}_2 = \left(\begin{bmatrix} 1 & 0 & 0 \\ 0 & r_{,\eta} r_{,\eta} & 0 \\ 0 & z_{,\eta} z_{,\eta} & 0 \\ 0 & r_{,\eta} z_{,\eta} & 0 \\ 0 & 0 & r_{,\eta} \\ 0 & 0 & z_{,\eta} \end{bmatrix} \right)\Big|_{\xi=\eta=0} \tag{51}$$

where

$\overline{\xi} = \dfrac{-r_1 + r_2 + r_3 - r_4}{3(r_1 + r_2 + r_3 + r_4)}$, $\overline{\eta} = \dfrac{-r_1 - r_2 + r_3 + r_4}{3(r_1 + r_2 + r_3 + r_4)}$ and $\langle f_1 \rangle = \langle f_2 \rangle = 0$ as posed by (12).

In particular, r_i denotes the radial coordinate of the i-th element node.

6. Numerical Examples

In this section, benchmark problems will be presented for the hybrid-stabilized piezoelectric elements. For convenience, the following abbreviations will be employed for the element models:

- PQ4 – the standard full-integrated (by 2nd order quadrature) four-node plane element.
- PQ4S – the hybrid-stabilized four-node plane element
- AQ4 – the standard full-integrated (by 2nd order quadrature) four-node axisymmetric element
- AQ4S – the hybrid-stabilized four-node axisymmetric element
- PQ9 – the standard full-integrated (by 3nd order quadrature) nine-node plane element
- PQ9S – the hybrid-stabilized nine-node plane element

Reduced-integrated elements are not considered due to the existence of the communicable zero energy modes. The piezoelectric material being considered is PZT-4 due to its popularity. When SI units are used to express its constitutive coefficients, the ratio of the most extreme coefficients can be as large as 10^{20} which may cause considerable round-off error in 8-byte or double precision

computation [30]. To avoid the error, the default units used for length, force, stress, charge, electric displacement and electric potential are taken to be respectively mm, N, N/mm^2, pC, pC/mm^2 and GV. In this light, the non-zero constitutive coefficients of PZT-4 (Park & Sun 1995) are:

$$c_{11} = c_{22} = 139\times10^3,\ c_{33} = 113\times10^3,\ c_{44} = c_{55} = 25.6\times10^3,\ c_{66} = 30.6\times10^3,$$
$$c_{12} = c_{21} = 77.8\times10^3,\ c_{13} = c_{31} = c_{23} = c_{32} = 74.3\times10^3 \text{ (in N/mm}^2\text{)};$$
$$e_{15} = e_{24} = 13.44\times10^6,\ e_{31} = e_{32} = -6.98\times10^6,\ e_{33} = 13.84\times10^6 \text{ (in pC/mm}^2\text{)};$$
$$\in_{11} = \in_{22} = 6.00\times10^9,\ \in_{33} = 5.47\times10^9 \text{ (in pC/(GVmm))}.$$

The electromechanical plane strain condition in which $\varepsilon_{zz} = E_z = 0$ will be assumed for the plane problems. With y- and z-axes taken to the poling directions for respectively plane and axisymmetric problems, the constitutive relations are:

$$\begin{Bmatrix} \sigma_x \\ \sigma_y \\ \tau_{xy} \\ D_x \\ D_y \end{Bmatrix} = \begin{bmatrix} c_{11} & c_{13} & 0 & 0 & e_{31} \\ c_{13} & c_{33} & 0 & 0 & e_{33} \\ 0 & 0 & c_{55} & e_{15} & 0 \\ 0 & 0 & e_{15} & -\in_{11} & 0 \\ e_{31} & e_{33} & 0 & 0 & -\in_{33} \end{bmatrix} \begin{Bmatrix} \varepsilon_x \\ \varepsilon_y \\ \gamma_{xy} \\ -E_x \\ -E_y \end{Bmatrix},$$

$$\begin{Bmatrix} \sigma_\theta \\ \sigma_r \\ \sigma_z \\ \tau_{zr} \\ D_r \\ D_z \end{Bmatrix} = \begin{bmatrix} c_{11} & c_{12} & c_{13} & 0 & 0 & e_{31} \\ c_{12} & c_{11} & c_{13} & 0 & 0 & e_{31} \\ c_{13} & c_{13} & c_{33} & 0 & 0 & e_{33} \\ 0 & 0 & 0 & c_{44} & e_{24} & 0 \\ 0 & 0 & 0 & e_{24} & -\in_{22} & 0 \\ e_{31} & e_{31} & e_{33} & 0 & 0 & -\in_{33} \end{bmatrix} \begin{Bmatrix} \varepsilon_\theta \\ \varepsilon_r \\ \varepsilon_z \\ \gamma_{zr} \\ -E_r \\ -E_z \end{Bmatrix} \tag{52}$$

7.1 Rank Tests

PQ4, PQ4S, PQ9, AQ4 and AQ4S possess only proper zero energy modes in which the electromechanical strain vanishes identically. PQ9S contains one spurious or improper zero energy mode. Though the electromechanical strain arising from the spurious zero energy mode does not vanish, the latter is incommunicable in the sense that it is self-suppressed when there are two or more elements in the same element assemblage.

7.2 Patch Test for Plane Elements

The 0.24×0.12 rectangular panel shown in Figure 2 is considered. All variables of the boundary nodes of the panel are prescribed in accordance with:

$$u_x = s_{11}\sigma_0 x \ , \ u_y = s_{13}\sigma_0 y \ , \ \phi = g_{31}\sigma_0 y \tag{53}$$

where σ_0 denotes a general stress value and other terms can be found in:

$$\begin{bmatrix} s_{11} & s_{13} & g_{31} \\ s_{13} & s_{33} & g_{33} \\ g_{31} & g_{33} & -f_{33} \end{bmatrix} = \begin{bmatrix} c_{11} & c_{13} & e_{31} \\ c_{13} & c_{33} & e_{33} \\ e_{31} & e_{33} & -\in_{33} \end{bmatrix}^{-1} \tag{54}$$

All predictions of PQ4, PQ4S, PQ9 and PQ9S conform to (53) and the related constant electromechanical stress and strain. In particular,

$$\sigma_x = \sigma_0 \ , \ \sigma_y = \tau_{xy} = D_x = D_y = 0 \, . \tag{55}$$

7.3 Patch Test for Axisymmetric Elements

In *r-z* coordinates, that patch in Figure 2 represents an annular with internal radius 0.2, external radius 0.44 and thickness 0.12. All variables of the boundary nodes of the annular are prescribed in accordance with:

$$u_r = \frac{-\sigma_0 r}{c_{11} + c_{12} + 2e_{31}^2 / \in_{33}} \ , \ u_z = 0 \, , \ \phi = \frac{-2e_{31}\sigma_0 z}{\in_{33} (c_{11} + c_{12}) + 2e_{31}^2} \tag{56}$$

where σ_0 is an arbitrary constant. All predictions of AQ4 and AQ4S conform to (56) and the related constant electromechanical stress and strain. In particular,

$$\sigma_r = \sigma_\theta = -\sigma_0 \ , \ \sigma_z = \frac{-2(c_{13} \in_{33} + e_{33} e_{31})}{\in_{33} (c_{11} + c_{12}) + 2e_{31}^2} \sigma_0 \ , \ \sigma_z = \tau_{zr} = D_r = D_z = 0 \, . \tag{57}$$

7.4 Bean Bending Test for Plane Elements

This example considers a cantilever of length (L) 10 and height (h) 2 modeled by two elements as shown in Figure 3. The cantilever is subjected to end bending. When the distortion parameter e vanishes, both elements are identical in geometry. The electric potential of all nodes at y = -1 are restrained to zero. The analytical solutions for the problem include:

$$u_x = -s_{11}\sigma_0 xy \ , \ u_y = \frac{s_{13}\sigma_0}{2}(\frac{h^2}{4} - y^2) + \frac{s_{11}}{2}\sigma_0 x^2 \, , \ \phi = \frac{g_{31}\sigma_0}{2}(\frac{h^2}{4} - y^2) \, , \ \sigma_x = -\sigma_0 y \ ,$$

$$\sigma_y = \tau_{xy} = D_x = D_y = 0 \, , \ M = \int_{-h/2}^{+h/2} y\sigma_x dz = -\frac{h^3\sigma_0}{12} = -hF \tag{58}$$

Figures 4 and 5 show the normalized deflections at A for four- and nine-node elements, respectively. It can be seen that PQ4S, PQ9 and PQ9S can reproduce the exact solution for e = 0. Moreover, both PQ4S and PQ9S are less susceptible to mesh distortion than PQ4 and PQ9, respectively.

7.5 Circular Plate Bending Test for Axisymmetric Elements

This example considers a circular plate of radius (R) 10 and thickness (h) 2 modeled by two elements as shown in Figure 3. The plate is subjected to radial end bending. When the distortion parameter e vanishes, both elements are identical in geometry in the r-z-plane. The electric potential of all nodes at z = -1 are restrained to zero. The analytical solutions for the problem include:

$$u_r = -(\overline{s}_{11} + \overline{s}_{12}) z r \sigma_0 \,,\; u_z = \overline{s}_{13}\sigma_0 (\frac{h^2}{4} - z^2) + \frac{\overline{s}_{11} + \overline{s}_{12}}{2}\sigma_0 r^2 \,,\; \phi = \overline{g}_{31}(\frac{h^2}{4} - z^2)\sigma_0 \,,$$

$$\sigma_r = \sigma_\theta = -z\sigma_0 \;,\; \sigma_z = \tau_{zx} = D_r = D_z = 0 \,,\; M_r\big|_{r=R} = 2\pi R \int_{-h/2}^{+h/2} z\sigma_r dz = -\frac{\pi R h^3 \sigma_0}{6} = -hF \,. \qquad (59)$$

where the undefined material coefficients can be found in:

$$\begin{bmatrix} \overline{s}_{11} & \overline{s}_{12} & \overline{s}_{13} & \overline{g}_{31} \\ \overline{s}_{12} & \overline{s}_{11} & \overline{s}_{13} & \overline{g}_{31} \\ \overline{s}_{13} & \overline{s}_{13} & \overline{s}_{33} & \overline{g}_{33} \\ \overline{g}_{31} & \overline{g}_{31} & \overline{g}_{33} & -\overline{f}_{33} \end{bmatrix} = \begin{bmatrix} c_{11} & c_{12} & c_{13} & e_{31} \\ c_{12} & c_{11} & c_{13} & e_{31} \\ c_{13} & c_{13} & c_{33} & e_{33} \\ e_{31} & e_{31} & e_{33} & -\in_{33} \end{bmatrix}^{-1}$$

Figure 6 shows the normalized deflections at A for four-node elements. For the considered range of e, AQ4 and AQ4S under- and over-predicts the deflection, respectively. However, AQ4S is less susceptible to mesh distortion and consistently more accurate than AQ4.

8. Closure

Based on the hybrid-stabilization method, this paper derives a four-node plane, a nine-node plane and a four-node axisymmetric stabilized elements for piezoelectric analysis. From the numerical examples, all the proposed elements are markedly more accurate and less susceptible to mesh distortion than their standard fully-integrated counterparts. Using the similar framework, a nine-node axisymmetric stabilized element has also been derived. However, the element is not apparently more accurate than the fully-integrated element and, thus, is not presented.

Acknowledgment – The financial support of *Research Grant Council of Hong Kong* (CERG: HKU 7082/97E) is gratefully acknowledged.

REFERENCES

1. A.Allik and T.J.R.Hughes, 'Finite element method for piezoelectric vibration', *Inter.J.Numer. Methods Engrg*., **2**, 151-157 (1970)
2. O.C.Zienkiewicz, R.L.Taylor. *The Finite Element Method*. 5th Edn. Butterworth-Heinemann, 2000.
3. M.Naillon, R.Coursant and F.Besnier, 'Analysis of piezoelectric structures by a finite element method', *Acta Electronica*, **25**, 341-362 (1983)
4. R.Lerch, 'Simulation of piezoelectric devices by two- and three-dimensional finite elements', *IEEE Trans. Ultrasonics, Ferroelectrics & Frequency Control*, **37**, 233-247 (1990)
5. N.-Q.Guo, P.Cawley and D.Hitchings, 'The finite element analysis of the vibration characteristics of piezoelectric disks', *J.Sound & Vibration*, **159**, 115-138 (1992)
6. W.-S.Hwang and H.C.Park, 'Finite element modeling of piezoelectric sensors and actuators', *AIAA J.*, **31**, 930-937 (1993)
7. M.A.Moetakef, K.L.Lawerence, S.P.Joshi and P.S.Shiakolas, 'Closed form expressions for higher order electroelastic tetrahedral elements', *AIAA J*. **33**, 136-142 (1995)
8. P.Heyliger, G.Ramirez and D.Saravanos, 'Coupled discrete-layer finite elements for laminated piezoelectric plates', *Commun. Numer.Methods Engrg*., **10**, 971-981 (1994)
9. H.S.Tzou and C.I.Tseng, 'Distributed piezoelectric sensor/actuator design for dynamic measurement/control of distributed parameter systems: a finite element approach', *J.Sound & Vibration*, **138**, 17-34 (1990)
10. R.Lammering, 'The application of a finite shell element for composites containing piezo-electric polymers in vibration control', *Computers & Structures*, **41**, 1101-1109 (1991)
11. S.K.Ha, C.Keilers and F.K.Chang, 'Finite element analysis of composite structures containing distributed piezoceramic sensors and actuators', *AIAA J*., **30**, 772-780 (1992)
12. H.S.Tzou, C.I.Tseng and H.Bahrami, 'A thin piezoelectric hexaxedron finite element applied to design of smart continua', *Finite Elements in Analysis & Design*, **16**, 27-42, (1994)
13. H.S.Tzou, R.Ye, 'Analysis of piezoelectric structures with laminated piezoelectric triangle shell element', *AIAA J*., **34**, 110-115 (1996)
14. J.Kim, V.V.Varadan and V.K.Varandan, 'Finite element modelling of structures including piezoelectric active devices', *Inter.J.Numer.Methods Engrg.,* **40**, 817-832 (1997)
15. D.A.Saravanos, P.R.Heyliger and D.H.Hopkins, 'Layerwise mechanics and finite element for the dynamic analysis of piezoelectric composite plates', *Inter.J.Solids & Structures*, **34**, 359-378 (1997)
16. K.Ghandi and N.W.Hagood, 'A hybrid finite element model for phase transitions in nonlinear electro-mechanically coupled material', *Smart Structures and Materials 1997: Mathematics and Control in Smart Structures*, ed. V.V.Varadan & J.Chandra, *Proc. SPIE*, **3039**, 97-112 (1997)
17. Sze KY, Pan YS. Hybrid piezoelectric finite element models for three-dimensional analysis. *J.Sound & Vibration*, **226**: 519-547 (1999)
18. Sze KY, Yao LQ, Yi S. A hybrid-stress ANS solid-shell element and its generalization for smart structure modelling – part II : smart structure modeling. *Inter.J.Numer.Methods Engrg*., **48**: 565-582 (2000)
19. Sze KY, Yao LQ. Modelling smart structures with segmented piezoelectric sensors and actuators. *J.Sound & Vibration*, **235**: 495-520 (2000)

20. Wu CC, Sze KY, Huang YQ. Numerical solutions on fracture of piezoelectric materials by hybrid element. *Inter.J.Solids & Structures*, **38**: 4315-4329 (2001)
21. E.P.EerNisse. Variational method for electroelastic vibration analysis. *IEEE Trans. Sonics and Ultrasonics*, **14**, 153-160 (1967)
22. Sze KY. Efficient formulation of robust hybrid elements using orthogonal stress/strain interpolants and admissible matrix formulation. *Inter.J.Numer.Methods Engrg.*, **35**: 1-20 (1992)
23. Sze KY. A novel approach for devising higher order hybrid elements. *Inter.J.Numer.Methods Engrg.*, **36**: 3303-3316 (1993)
24. Sze KY, Fan H, Chow CL. Elimination of spurious kinematic and pressure modes in biquadratic plane element. *Inter.J.Numer.Methods Engrg*., **38**: 3911-3932 (1995)
25. Sze KY. Admissible matrix formulation : from orthogonal approach to explicit hybrid-stabilization. *Finite Elements in Analysis & Design*, **24**: 1-30 (1996)
26. Sze KY, Chow CL, Chen W-J. Improved formulations of Q_{cs6} hybrid element in computational efficiency. *Inter.J.Numer.Methods Engrg.*, **31**: 999-1008 (1991)
27. T.H.H.Pian, "Finite elements based on consistently assumed stresses and displacements", *Finite Elements in Analysis & Design*, **1**, 131-140 (1985)
28. Sze KY, Chow CL. An incompatible element for axisymmetric structure and its modification by hybrid method. *Inter.J.Numerical Methods Engrg.*, **31**: 385-405 (1991)
29. Weissman SL, Taylor RL. Four-node axisymmetric element based upon the Hellinger-Reissner functional. *Computer Methods Appl.Mech. & Engrg.*, **85**: 39-55 (1991)
30. Sze KY, Wang HT, Fan H. A finite element approach for computing edge singularities in piezoelectric materials. *Inter.J.Solids & Structures*, **38**: 9233-9252 (2001)
31. Park SB, Sun CT. Effect of electric field on fracture of piezoelectric ceramics. *Inter.J.Fract*, **70**: 203-216 (1995)

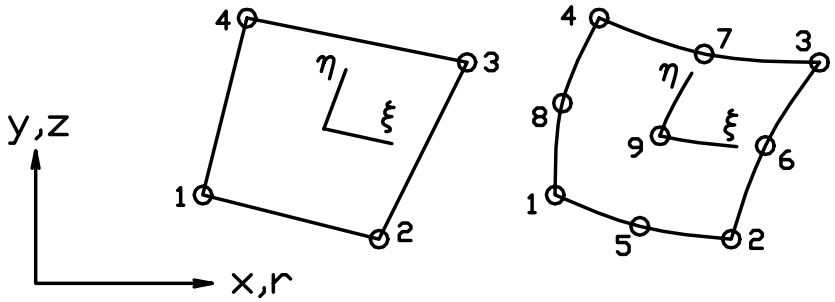

Figure 1. Four-node and nine-node quadrilateral elements.

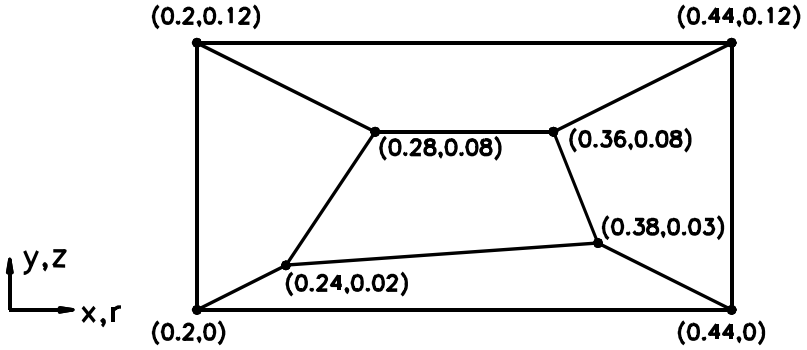

Figure 2. Mesh for rectangular panel and annular ring.

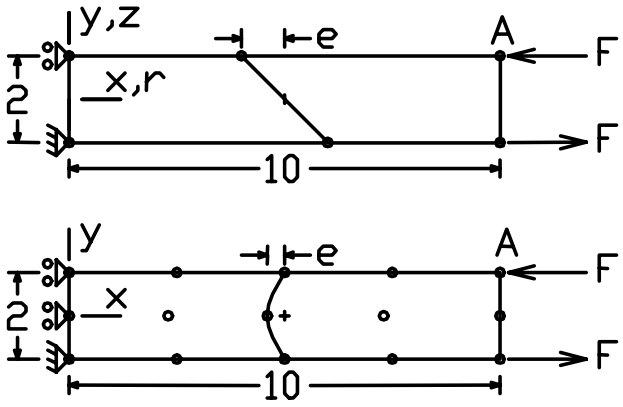

Figure 3. Two-element meshes with distortion featured by “e”.

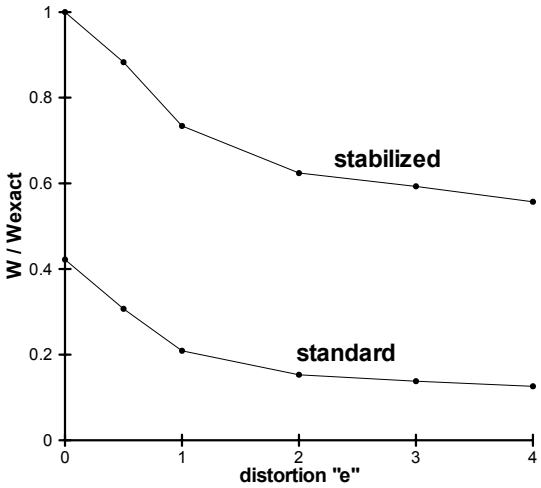

Figure 4. Normalized deflection predictions at A by four-node plane elements, see Figure 3.

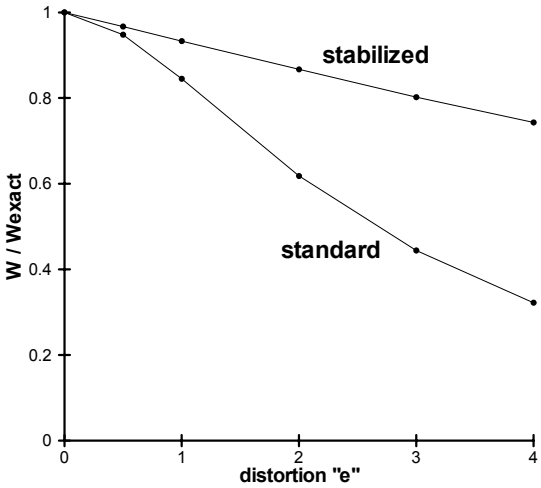

Figure 5. Normalized deflection predictions at A by nine-node plane elements, see Figure 3.

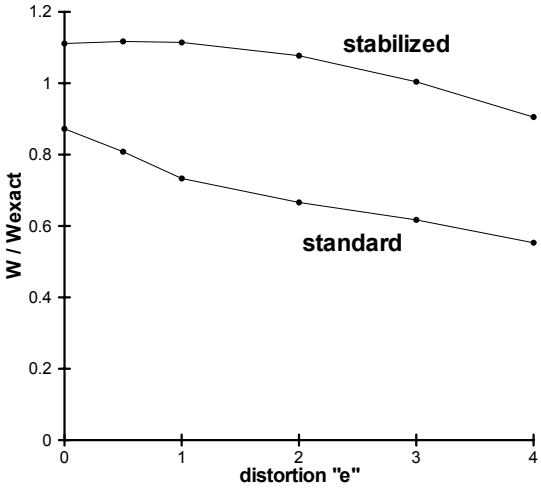

Figure 6. Normalized deflection predictions at A by four-node axisymmetric elements, see Figure 3.